iJRASET
International Journal For Research in Applied Science and Engineering Technology

INTERNATIONAL JOURNAL FOR RESEARCH

IN APPLIED SCIENCE & ENGINEERING TECHNOLOGY

Volume: 10 **Issue:** X **Month of publication:** October 2022

DOI: https://doi.org/10.22214/ijraset.2022.47051

www.ijraset.com

Call: 08813907089 | E-mail ID: ijraset@gmail.com

International Journal for Research in Applied Science & Engineering Technology (IJRASET)
ISSN: 2321-9653; IC Value: 45.98; SJ Impact Factor: 7.538
Volume 10 Issue X Oct 2022- Available at www.ijraset.com

Oblate Distorted Harmonic Oscillator Symmetry

Aum Rawal
Science and Technology, University of debrecen, Debrecen-4032, Hungary

Abstract: ***Harmonic oscillator states have shown advantageous for nuclear structure. Nuclear physics experts have developed sophisticated group theory-based mathematical techniques to handle n-particle states in the harmonic oscillator (ho) potential as a result of this. The deformed harmonic oscillator (HO)'s oblate shell closure has been studied, and the results demonstrate that the accompanying magic numbers are connected to a universal sequence of the triangular numbers that identically characterize oblate, spherical, and prolate. This offers a distinct framework for comprehending the distorted HO. There is discussion of the effects on oblate nuclei in the present study. The current work examines the symmetries of the deformed HO on the oblate side of deformation and demonstrates that these spherical degeneracies are equally important on this side of deformation as they are on the prolate side. The significance of these symmetries for comprehending nuclear structure is highlighted.***
Keywords: Harmonic Oscillator; Oblate; Deformation; Nuclear Clustering.

I. INTRODUCTION

The nuclear structure has benefited from harmonic oscillator states. This has prompted experts in nuclear physics to create complex group theory-based mathematical methods for handling n-particle states in the harmonic oscillator (ho) potential. The potential can be distorted and oscillation frequencies can vary along the three-axis of Cartesian coordinate directions thanks to the three-dimensional HO. When the system is constrained, the deformation along one of the axis is changed but the deformation in the other remaining Cartesian directions is kept constant and equal, this is known as axially symmetric deformation. The ensuing deformations are either of the oblate or prolate types, depending on whether the deformation along one axis is longer or shorter than in the other directions. The distorted HO's solution as a result of this distortion is shown in Figure 1.

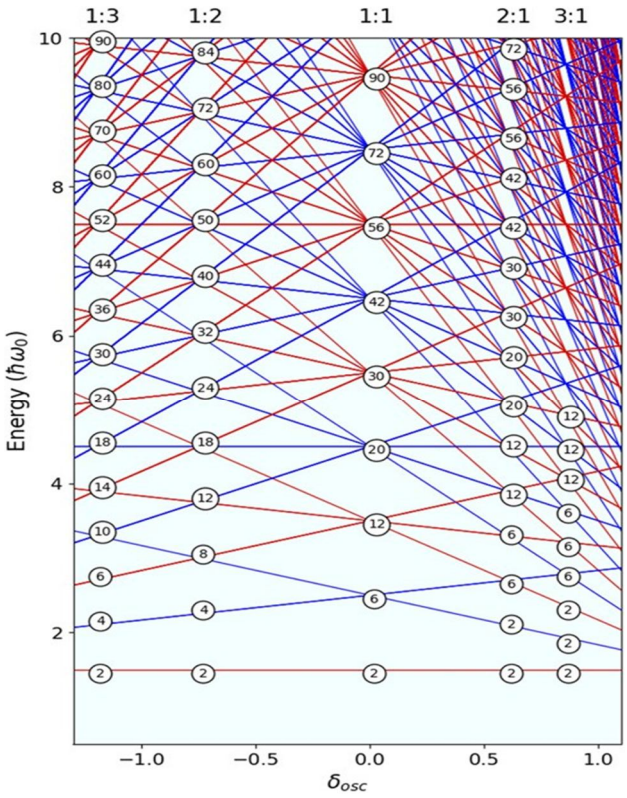

Figure 1: Levels of energy in the distorted HO

ISSN: 2321-9653; IC Value: 45.98; SJ Impact Factor: 7.538
Volume 10 Issue X Oct 2022- Available at www.ijraset.com

Equation gives the energy levels of the distorted HO. n_x, n_y, and n_z are the oscillator quantum in each direction of the Cartesian coordinate system (CCS), and x, y, and z are the fundamental frequencies of oscillation, with 0 being equal to $(n_x + n_y + z)/3$. For axial geometry, where $\omega_x = \omega_y = \omega_\perp$, the z-axis is assumed to be the primary deformation axis. The parameter for deformation is then determined by equation (2), where the axial length deformations def_z:$def_\perp$, 2:1 and 3:1 correspond to osc = 0.6 and 0.86 and $\omega_\perp$:ω_z = 2:1 and 3:1, respectively.

$$E = \hbar w_x n_x + \hbar w_y n_x + \hbar w_z n_z + \frac{3}{2}\hbar w_o \quad (1)$$

$$\delta_{osc} = \frac{(w_\perp - w_z)}{w_o} \quad (2)$$

The distorted HO has provided significant insight into the physics of nuclei since the solutions to the Schrödinger equation offer a decent approximation to the more precise flat-bottomed nuclear potentials that describe the mean-field in which the nucleons flow [1-4]. The resultant shell structure produces a series of magic numbers as the potential is distorted. At integer ratios of axial deformation, the shell structure which is present at zero deformation returns. This generates brand-new magic number sequences for each deformation. Despite the fact that group theory techniques have often been used to define these magic numbers and the resulting degeneracies, a general group theory description that accounts for both oblate and prolate deformations has not yet been established [5].

It is well-known how prolate deformed nuclei appear, as well as how super-deformation and clustering manifest [2, 3]. The axial deformations of def_z: $def_\perp$ of 2:1 and 3:1 between shell gap is shown in figure 1 and are connected to a series of spherical degeneracies (2, 6, 12, 20, 30,) that repeat multiple times such as twice or thrice. Accordingly, Rae [6] showed that ^{8}Be can be explained by two α-particle clusters, ^{20}Ne ^{16}O +α, etc. In other words, two spherical clusters provide clusterization at a prolate deformation of 2:1. Experimental observations [7] confirm these conclusions.

The oblate structures of the nuclei ^{12}C and ^{28}Si have been related to underlying cluster symmetries via anti-symmetrized molecular dynamics (AMD) [11] and the alpha cluster model [10] and, which were both published. Similar to this, modern computations using relativistic and non-relativistic density functional techniques [12, 13] also reveal cluster structure. Three α -clusters with a D_{3h} symmetry are thought to have created the 12C nucleus [14, 15]. Similar to this, a 7-pentagonal configuration with D_{5h} symmetry can be connected to the $K^\pi = 5^-$ band in ^{28}Si [11]. Oblate shapes are known to contribute to the phenomena of shape co-existence in heavier systems, where oblate and prolate shapes' deformation energies are comparable and the nucleus can transition between them by tunneling through the intermediary barrier [16]. Oblate structures hence function from light to heavy nuclei. The symmetries of the deformed HO on the oblate side of deformation are examined in the current work, and it is shown that these spherical degeneracies are just as significant as they are on the prolate side of deformation. It is discussed how important these symmetries are for understanding nuclear structure.

II. THE OBLATE SYMMETRIES AND THE DISTORTED HO

The levels of energy in the distorted HO are shown in Figure 1. Equation (1) governs how the energy levels are ordered. The energy levels and $\delta_{osc} = 0$, $\omega_x = \omega_y = \omega_z$ are separated in energy by $\hbar w_o$ for zero deformation, and the degeneracies for neutrons/protons spin up and down are 2, 6, 12, 20, 30, 42, etc. The resulting numbers are 2, 8, 20, 40, 70, and 112. (Total degeneracy) The shell structure (which is a region of high degeneracy) primarily disappears for prolate deformations, as mentioned above, Moreover, the level structure gets more intricate. At integer ratios of the z-deformation direction's lengths to the transverse directions, the shell structure returns., such as 2:1, 3:1, 4:1, etc. At 2:1, 3:1, and 4:1, the spherical degeneracy pattern is reproduced twice, three times, and four times.

On the oblate side of deformation, there is furthermore a shell structure, where $\delta_{osc} < 0$, but neither the shell structure nor the underlying degeneracies have been given a straightforward explanation [5], which is the aim of the current investigation. The sequence of degeneracies at an oblate deformation of 1:2 ($\delta_{osc} = 0.75$) is 2, 4, 8, 12, 18, 24,..., (Fig. 1)and at 1:3 (osc = 1.2), they are 2, 4, 6, 10, 14, 18, 24, and so on. These degeneracies can be broken down into the sequences 1:2: 2 + 0, 2 + 2, 6 + 2, 6 + 6, 12 + 6, 12 + 12, and 1:3: 2 + 0 + 0, 2 + 2 + 0, 2 + 2 + 2, 6 + 2 + 2, 6 + 6 + 2, 6 + 6 + 6, 12 + 6 + 6 (Fig. 2). Thus, it can be shown that the prolate and oblate sides of deformation are also affected by the spherical degeneracies. This straightforward discovery suggests a way to reinterpret the deformed HO's energy level scheme in reference to the series of spherical degeneracies, as depicted in figure 3. One observes that the complete level system, from spherical to prolate and oblate deformations, may be recreated by a single succession of spherical degeneracies.

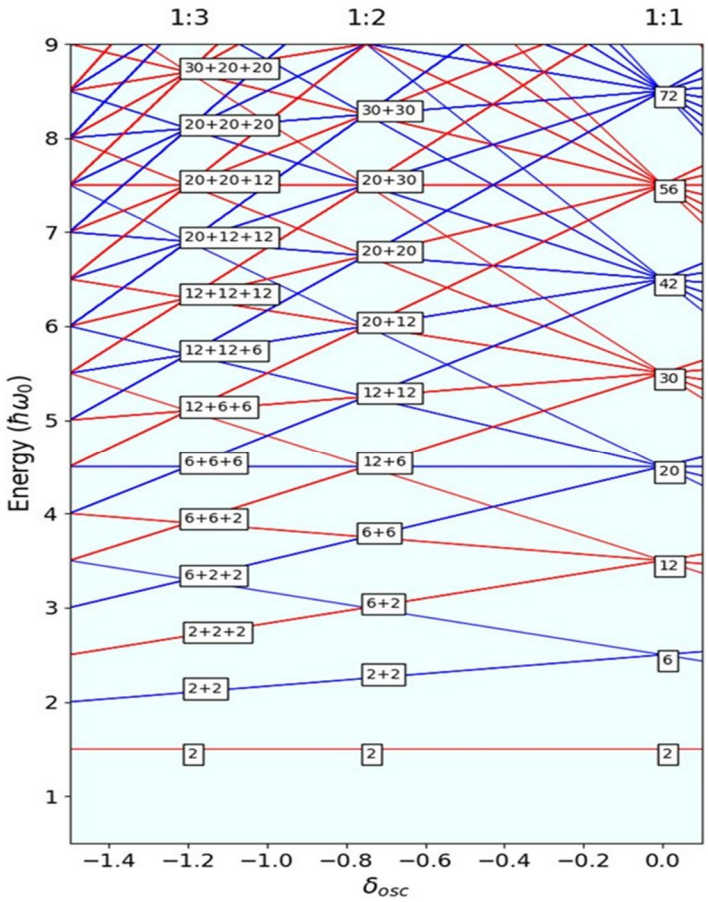

Figure 2: The distorted HO's oblate side

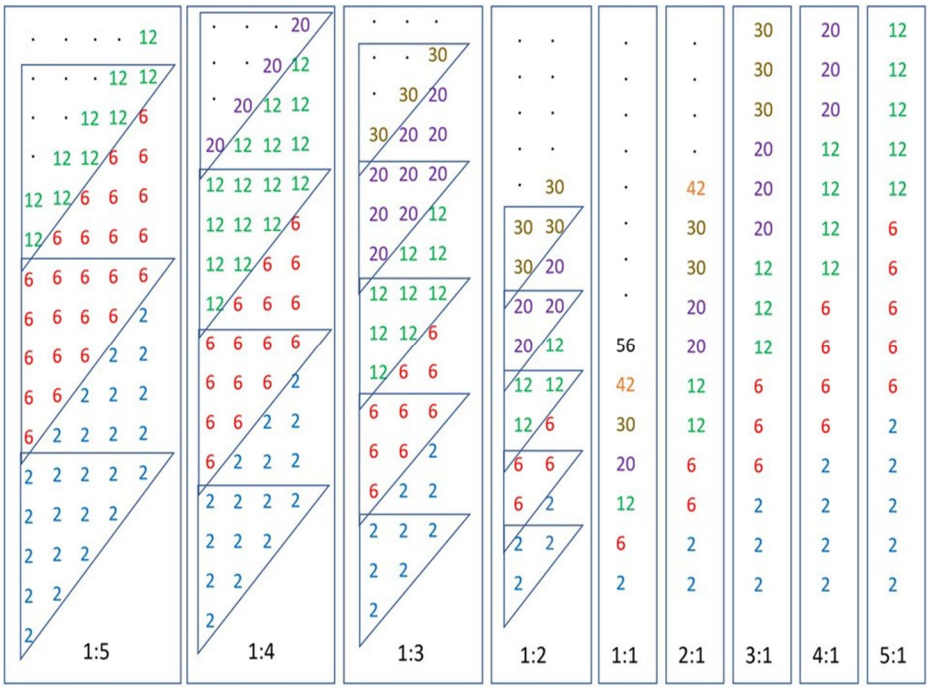

Figure 3: The degeneracy pattern of the distorted HO

ISSN: 2321-9653; IC Value: 45.98; SJ Impact Factor: 7.538
Volume 10 Issue X Oct 2022- Available at www.ijraset.com

The Harvey model or alternatively the two-centered oscillator framework can be used to analyze the patterns seen in figure 3 [17]. One starts by taking into account prolate deformations. The merging of different configurations of HO clusters into the composite system can be taken into consideration in both descriptions. The original two degenerate energy levels for HO (n_x, n_y, n_z) evolve into the two different levels (n_x, n_y, $2n_z$) and (n_x, n_y, $2n_z + 1$) if these clusters are fused by their respective motion down the z-axis. These guidelines apply to Harvey. They may be described by considering the properties of wavefunctions along the z-axis, where the number of nodes is preserved or an additional node is produced by inverting one wavefunction, i.e., equation (3)

$$= \frac{\varphi_1 \pm \varphi_2}{2} \quad (3)$$

Three degenerate levels (n_x, n_y, n_z) for three centers evolve to (n_x, n_y, $3n_z$), (n_x, n_y, $3n_z + 1$), and (n_x, n_y, $3n_z + 2$), etc. As a result, the three primarily distinct and degenerate (0, 0, 0) levels for three centers become (0, 0, 0), (0, 0, 1), and the energy separation for these is 1 $\hbar w_o$ because the Δn_z is 1. Given that $\omega_\perp/\omega_z = 3$, the energy of the (0, 0, 0), (0, 0, 1), and (0, 0, 2) levels is lower (0 $\hbar w_z$, 1 $\hbar w_z$, and 2 $\hbar w_z$, respectively) than that of the (1, 0, 0) and (0, 1, 0) levels (see figure 1), which are degenerate, with the (0, 0, 3) level (3 $\hbar w_z$) having the lowest energy degeneracy of 6 at 3:1. According to the rules, combining the levels represented by the order of degeneracies (2, 6, 12, 20, 30) + (2, 6, 12, 20, 30...) + (2, 6, 12, 20, 30) elevates each of the three results by 0 $\hbar w_z$, 1 $\hbar w_z$, or 2 $\hbar w_z$ without affecting the common degeneracy values, i.e. the sequence (2, 2, 2, 6, 6, 6, 12, 12,...) results. In the most straightforward scenario, the fusing of two α-particles, (0, 0, 0), results in the production of an ^{8}Be nucleus with populated (0, 0, 0) and (0, 0, 1) levels, which is certainly what would be predicted for a 2:1 prolate deformation from figure 1.

Turning now to the oblate side. The sequences in figure 3 can be interpreted in the manner described below. At a deformation of 1:2, two prolate nuclei are oriented with the deformation axis aligned with the x-axis and separated by the y-coordinate, that is, with the deformation axes perpendicular to the z-axis. The sequence (2, 2, 6, 6, 12, 12) can be used to represent each nucleus, but the x-axis serves as the representative deformation coordinate. According to the Harvey rules, when the two sequences are fused along the y-axis, one has energy added of 0 $\hbar w_\perp$ and the other of 1 $\hbar w_\perp$. Given that the sequence (2, 2, 6, 6, 12, 12)'s levels are separated by 1 $\hbar w_\perp$ the new sequence in the composite system is (2, 2 + 2, 6 + 2, 6 + 6, 12 + 6, 12 + 12).

III. CHARACTERISTICS

There are two new traits. The spherical degeneracies originate from the triangle-shaped integers themselves. The production of nuclei like ^{16}O from eight neutrons and eight protons results in a tetrahedron of four -particles since each level may store two paired neutrons and two paired protons.

The triangle accommodating six particles is added to the base of the ^{16}O tetrahedron in the subsequent shell closure, resulting in the construction of the ^{40}Ca tetrahedron. Referral [9] has been used to explain this. However, as seen by the triangles displayed in figure 3, other triangular structures also exist in the oblate nucleus.

Three α-particles (^{12}C) complete the first triangle if one uses the example of nuclei with a distortion of 1:2. In the square matrix depicted in figure 4, this would translate to three of the four corners being occupied and the fourth corner being empty. A ^{16}O cluster is completed at one corner and a α-particle is added to the fourth corner by the following shell closure at 1:2 (6 + 2). Two more original -particles are subsequently converted to ^{16}O nuclei by the subsequent shell closure (6 + 6), resulting in a 3*^{16}O triangle and one more α-particle.

Contour plots for density obtained in the x-y plane are used in Figure 4 to show how alternative cluster configurations within that plane were fused using the Harvey criterion. (top) three prolate distorted 3:1 nuclei, two prolate deformed 2:1 nuclei, and four prolate deformed 4:1 nuclei fused. The α-particles are depicted by the green dots. The charts display the densities related to the HO configurations, which are supplied for the composite system. (bottom) The same as before, but with the harmonic configurations (0, 0, 0), (1, 0, 0), and (0, 0, 1) described by the Harvey rules; each red dot denotes the geometric position of a ^{16}O cluster prior to the application of the Harvey rules. In light of this, the sequence for the deformation in oblate structure of 1:2 can be explained by means of construction of 3-centers with degeneracy of 2, 6, and 12, or, alternatively, by creating triangles from initial α- particles, then ^{16}O, and finally ^{40}Ca clusters. The three centers in figure 4 are connected to three of the square's four corners. For example, for three ^{16}O clusters, the fourth is an α-particle. The cluster, which is one smaller, is located in the fourth corner. Three -particles are the special case, and in ^{12}C, the fourth slot is unoccupied. Three times this results in triangles with six centers (plus three centers occupied by the lighter cluster), four times this results in triangles with ten centers (plus six centers occupied by the lighter cluster), and five times this results in triangles with fifteen centers (plus ten centers occupied by the lighter cluster), all of which are triangular numbers.

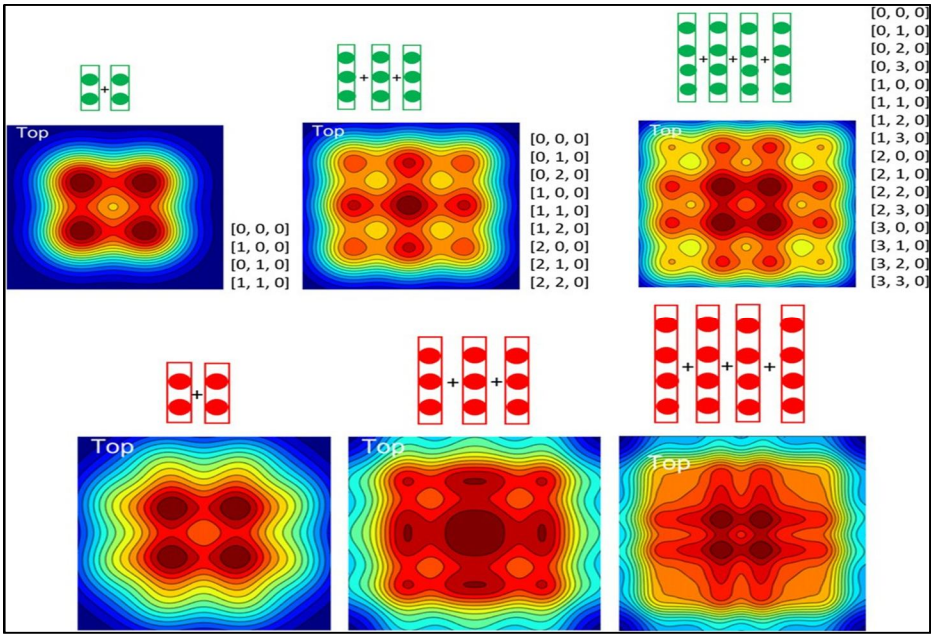

Figure 4: Plots of density calculated in the x-y plane

The pattern is compelling because of how straightforward it is, but it might just be a coincidence, and there may be other approaches to explaining the magic numbers nature that emerges in the warped HO. By looking at the symmetries of the densities that may be derived from the HO wavefunctions, the robustness of the current approach can be put to the test. As was done in [3], these different densities were created by adding the probabilities of the levels equal to the shell closure. Figures 5 and 6 indicate the order in which the orbits get degenerated at 1:3 and 1:2 and are how it gets filled afterward, which is depicted in picture 4.

Figure 5 depicts the accomplishment of the three-center system equal to the degeneracy number of 20, or 140 neutrons and 140 protons, or the full spectrum of nuclei, constructed from the most basic ^{12}C to the most complicated. In order to take into account, the volume changes, as well as the r2 dependence of the HO potential, the density plots' horizontal and vertical axes, have been scaled according to the ratio $A^{1/6}$ (where A is the number of nucleons). This makes it possible to compare the densities side by side. Simple observations to be made are as follows: (i) Axial symmetry exists at all densities (This is destroyed by even one level being removed from the computation.), (ii) There is always a dip in the center density (top) for the triangle closure, and the density profile in the transverse direction (side) has a fairly uniform vertical dimension. (iii) and for the partially accommodated triangles, there is a peak near the central density and a bulge along the axis in the side profile. As anticipated by the symmetries spanning this spectrum of magic numbers, it's observed that the symmetries found in these densities are repeated in synchronicity. In figure 5, Densities are estimated at a ratio of 1:2 by adding each unique density up to the arrow-indicated point. In each case, side and top profiles are displayed. The density calculations' inclusion of various energy levels is indicated by the red values.

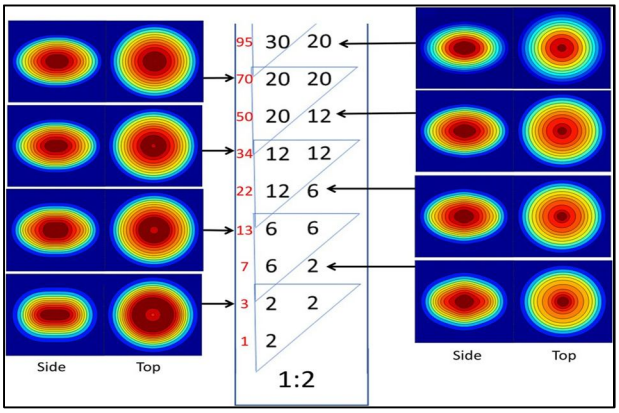

Figure 5: Densities at the deformation of 1:2

Although the central dip in the closed triangle is no longer present, the oblate 1:3 density, shown in figure 6, nevertheless exhibits a similar pattern. This dip comes back at a ratio of 1:4, making it a feature that changes as the deformation increases. It is important to note that the degree of agreement is not insignificant and that changes to the single particle designs have a significant influence on densities. Thus, this symmetry is solid.

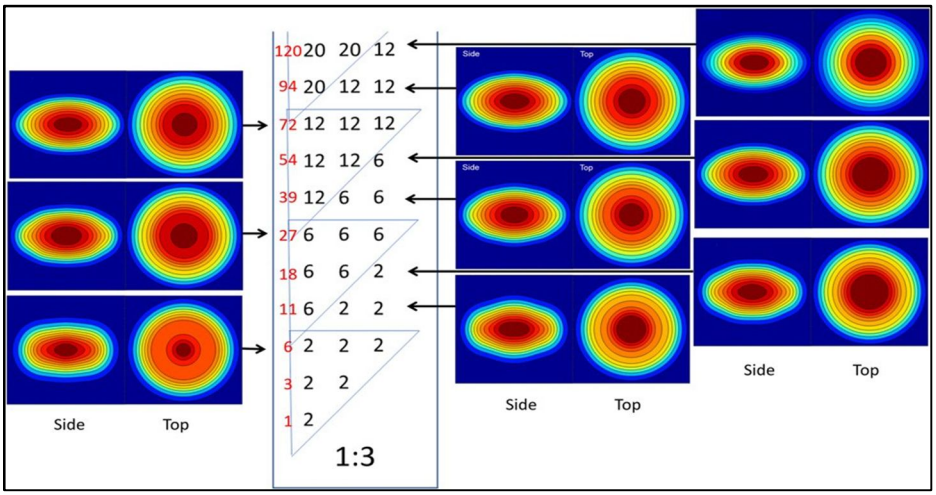

Figure 6: Densities at the deformation of 1:3

IV. CONCLUSION

The current study uncovers a fresh framework for comprehending the distorted HO in reference to a single order of triangular numbers that are, 2, 6, 12, 20, 30… which connects the structures throughout all different deformations, from oblate to prolate. The stacking of -particle triangular structures and the subsequent degeneracy sequences 2, 6, 12, 20, 30, can be used to explain the symmetries of spherical nuclei. While nuclei connected to prolate shell closures during deformations in order of N:1 are associated with N spherical clusters, oblate nuclei during deformations in order of 1: N may be described in terms of the assembling of spherical-shaped clusters into a square-shaped N×N matrix. Symmetries are still important for nuclei in more unusual deformations, but these structures will only be seen at high excitation energies since their associated states will fragment due to coupling with the background of other states.

The question of whether the symmetries discovered in the current computations endure the stimulus of the spin-orbit interactions and Coulomb consequently have any impact on actual nuclei is another concern. Some solace may be taken in the fact that the shell structures seen in one are also seen in the other, and that the DHO and Nilsson level schemes are relatively equivalent for light nuclei. The AMD method, which employs genuine nucleon-nucleon interactions as demonstrated for 12C and 28Si, yields outcomes that are equivalent to those of more basic nuclear models, demonstrating once more that the ideas discussed here do in fact guide the behavior in these more complex nuclear models. It would be desirable to do a more thorough investigation of how the discovered symmetries affect microscopic nuclear models. However, it should not be interpreted that the ideas presented here interpret nuclei in respect of a crystalline structure of the clusters. Instead, they display a number of symmetries that have a big impact on how nuclei are structured. These symmetries may also be useful for group theory approaches to the distorted HO's energy level scheme.

REFERENCES

[1] Nazarewicz W and Dobaczewski J 1992 Phys. Rev. Lett. 68 154
[2] Freer M, Betts R R and Wuosmaa A H 1995 Nucl. Phys. A 587 36
[3] Bengtsson T, Faber M E, Leander G, Möller P, Ploszajczak M, Ragnarsson I and Åberg S 1981
[4] Phys. Scr. 24 200
[5] Nazarewicz W, Dobaczewski J and Van Isacker P 1992 AIP Conf. Proc. 259 30
[6] Rae W D M 1988 Int. J. Mod. Phys. A 03 1343
[7] Freer M 2007 Rep. Prog. Phys. 70 2149
[8] Canavan R and Freer M 2020 J. Phys. G: Nucl. Part. Phys. 47 095102
[9] Rae W D M and Zhang J 1994 Mod. Phys. Lett. A 09 599
[10] Brink D M 1966 Proc. Int. School of Physics Enrico Fermi vol 36 ed C Bloch (New York: Academic) p 247
[11] Tumino, R. Bijker, and F. Iachello, in Clustering Aspects of Nuclear Structure and Nuclear Dynamics, edited by M. Korojila, Z. Basrak, and R. Caplar (World Scientific, Singapore, 2000), p. 271.

[12] M. Freer et al., Phys. Rev. C 76, 034320 (2007).
[13] O. S. Kirsebom et al., Phys. Rev. C 81, 064313 (2010).
[14] F. Iachello, Phys. Rev. C 23, 2778(R) (1981).
[15] M. Gai, M. Ruscev, A. C. Hayes, J. F. Ennis, R. Keddy, E. C. Schloemer, S. M. Sterbenz, and D. A. Bromley, Phys. Rev. Lett. 50, 239 (1983).
[16] R. Bijker and F. Iachello, Phys. Rev. Lett. 112, 152501 (2014).
[17] R. Roth, J. Langhammer, A. Calci, S. Binder, and P. Navratil, Phys. Rev. Lett. 107, 072501 (2011).
[18] A. C. Dreyfuss, K. D. Launey, T. Dytrych, J. P. Draayer, and C.Bahri, Phys. Lett. B 727, 511 (2013).
[19] E. Epelbaum, H. Krebs, D. Lee, and U.-G. Meissner, Phys. Rev. Lett. 106, 192501 (2011); E. Epelbaum, H. Krebs, T. A. Lahde, D. Lee, and U.-G. Meissner, Phys. Rev. Lett. 109, 252501 (2012).
[20] M. Kamimura, Nucl. Phys. A351, 456 (1981).
[21] Y. Kanada-Enyo, Prog. Theor. Phys. 117, 655 (2007).
[22] M. Chernykh, H. Feldmeier, T. Neff, P. von Neumann Cosel, and A. Richter, Phys. Rev. Lett. 98, 032501 (2007).
[23] Y. Funaki, H. Horiuchi, W. von Oertzen, G. Ropke, P. Schuck, A. Tohsaki, and T. Yamada, Phys. Rev. C 80, 064326 (2009) and references therein.

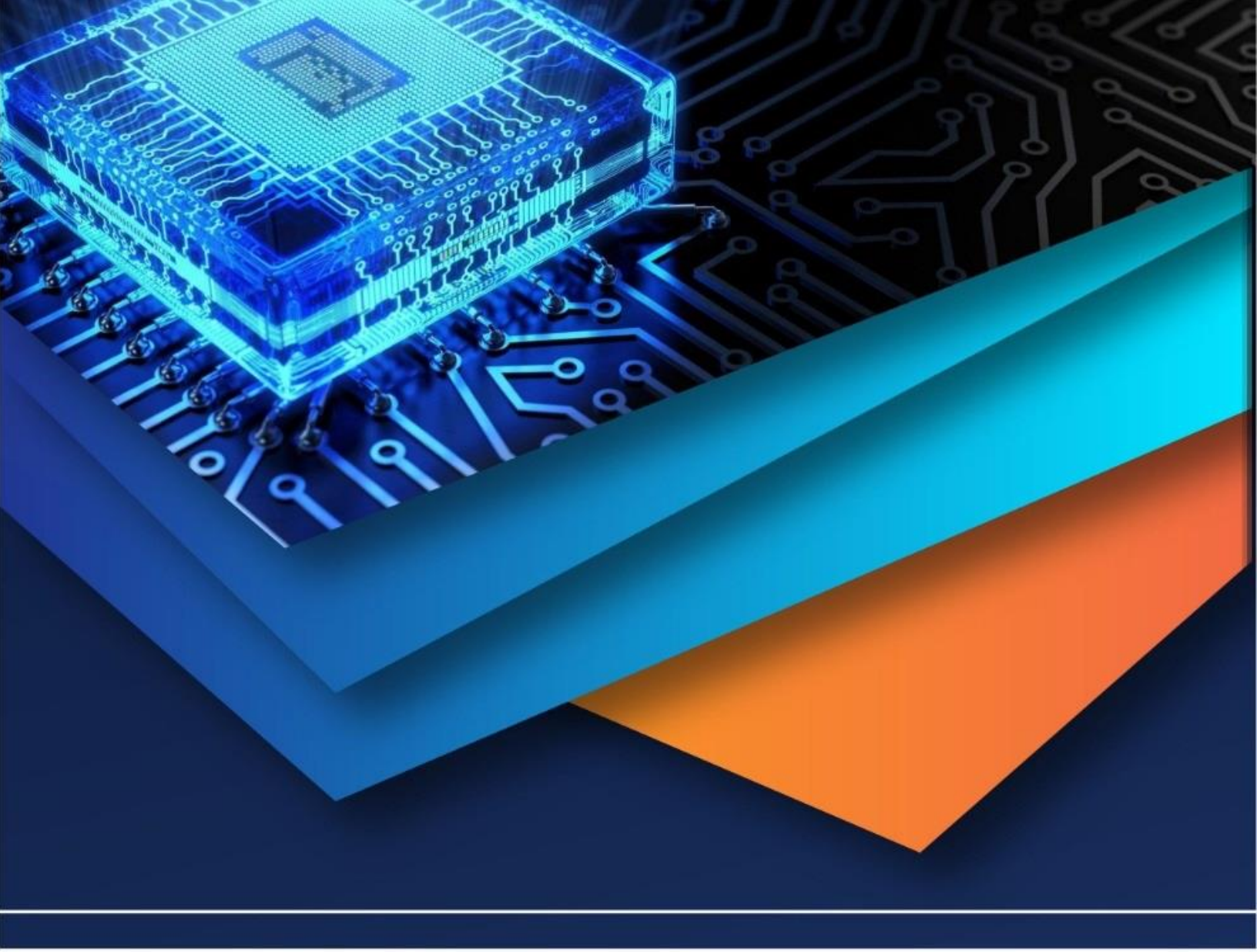

10.22214/IJRASET

45.98

IMPACT FACTOR: 7.129

IMPACT FACTOR: 7.429

INTERNATIONAL JOURNAL FOR RESEARCH

IN APPLIED SCIENCE & ENGINEERING TECHNOLOGY